Two-level systems driven by large-amplitude fields

S. Ashhab,[1] J. R. Johansson,[1] A. M. Zagoskin,[1,2] and Franco Nori[1,3]

[1]*Frontier Research System, The Institute of Physical and Chemical Research (RIKEN), Wako-shi, Saitama 351-0198, Japan*
[2]*Department of Physics and Astronomy, The University of British Columbia, Vancouver, BC, Canada V6T 1Z1*
[3]*Physics Department and Michigan Center for Theoretical Physics, The University of Michigan, Ann Arbor,
Michigan 48109-1040, USA*

We analyze the dynamics of a two-level system subject to driving by large-amplitude external fields, focusing on the resonance properties in the case of driving around the region of avoided level crossing. In particular, we consider three main questions that characterize resonance dynamics: (1) the resonance condition, (2) the frequency of the resulting oscillations on resonance, and (3) the width of the resonance. We identify the regions of validity of different approximations. In a large region of the parameter space, we use a geometric picture in order to obtain both a simple understanding of the dynamics and quantitative results. The geometric approach is obtained by dividing the evolution into discrete time steps, with each time step described by either a phase shift on the basis states or a coherent mixing process corresponding to a Landau-Zener crossing. We compare the results of the geometric picture with those of a rotating wave approximation. We also comment briefly on the prospects of employing strong driving as a useful tool to manipulate two-level systems.

I. INTRODUCTION

Two-level systems are ubiquitous in various fields of physics. A large number of quantum phenomena rely on the existence of two quantum states, or their underlying principles can be understood using the simple model of a two-level system. Recently, two-level systems have gained renewed attention as they represent the building blocks for quantum information processing (QIP) applications [1].

In the study of two-level systems, as well as many other quantum systems, avoided level crossings are associated with a wide variety of interesting phenomena. Large amounts of literature have been devoted to analyzing the dynamics of a two-level system driven around an avoided crossing, particularly in connection with Landau-Zener (LZ) physics [2]. These avoided crossing regions have a special significance in QIP applications because coherence times are usually longest in those regions, hence the term optimal point. Needless to say, nontrivial evolution of quantum systems is usually associated with some kind of energy-level crossing.

In this paper we discuss the dynamics of a two-level system driven by strong ac fields in the vicinity of an avoided crossing. As mentioned above, numerous studies have been devoted to this problem, approaching it from different angles and applying it to different physical systems. Here we present a geometric picture that leads to a simple understanding of the behavior of the system. This approach can also be used to derive quantitative results in regions where other methods fail. We also keep in mind the idea of trying to find useful applications for strong driving as a tool to manipulate two-level systems, or as they are referred to in the context of QIP, qubits (in this context see, e.g., [3,4]).

A good example displaying the richness of strongly driven two-level systems is the so-called coherent destruction of tunnelling (CDT) [5]. A particle in a symmetric double-well potential will generally oscillate back and forth between the two wells. If we now add an oscillating energy difference

between the two wells, the frequency of the tunnelling oscillations changes. At certain combinations of the driving parameters, the tunnelling oscillations are frozen. This phenomenon has been analyzed from several different perspectives [6–11]. We shall show below that it can be understood rather easily using our approach.

Here we consider the situation where we start with an undriven system at an arbitrary bias point. We then analyze the dynamics that results from the application of strong driving fields. As one would expect, resonance peaks occur at properly chosen values of the parameters. We analyze the resonance conditions using two approaches: one employing a rotating wave approximation (RWA) and one employing an approximation of discretized evolution characterized by a sequence of fast LZ crossings. Between the two approaches, and the well-known weak-driving case, most of the parameter space is covered.

This paper is organized as follows. In Sec. II we present the model system, the Hamiltonian that describes it and some preliminary arguments. In Sec. III we present a RWA that can be used to describe the dynamics in a certain region of the parameter space. In Sec. IV we present a geometric picture that is useful to describe the dynamics in another region of the parameter space (note that there is some overlap between the validity regions of Secs. III and IV). Section V contains a discussion of the results and some concluding remarks.

II. MODEL SYSTEM AND HAMILTONIAN

We consider a two-level system described by the Hamiltonian

$$\hat{H}(t) = -\frac{\Delta}{2}\hat{\sigma}_x - \frac{\epsilon(t)}{2}\hat{\sigma}_z. \tag{1}$$

where Δ is the (time-independent) coupling strength between the two basis states [12]; $\epsilon(t)$ is the time-dependent bias
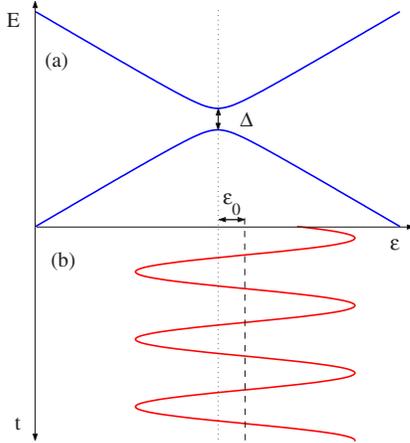
FIG. 1. (Color online) (a) Energy-level diagram $E(\epsilon)$ [solid lines (blue)] of a two-level system with minimum gap Δ and (b) the time-periodic bias $\epsilon(t)$ [solid line (red)]. The vertical dashed line represents dc bias point ϵ_0.

point; and $\hat{\sigma}_x$ and $\hat{\sigma}_z$ are the usual x and z Pauli matrices, respectively. Note that we take $\hbar=1$ throughout this paper. For definiteness and simplicity in the algebra, we assume harmonic driving, i.e., we assume that $\epsilon(t)$ can be expressed as

$$\epsilon(t) = \epsilon_0 + A\cos(\omega t + \phi), \qquad (2)$$

where ϵ_0 is the dc component of the bias point; and A, ω, and ϕ are, respectively, the amplitude, frequency, and phase of the driving field. We shall, with no loss of generality, take all the parameters in Eqs. (1) and (2) to be positive. In order to simplify the appearance of the expressions below, we shall take $\phi=0$. This only simplifies the intermediate steps of the algebra, but it does not affect any of the main results. The energy-level diagram and the applied driving field are depicted in Fig. 1.

We should mention here that recently this setup was studied experimentally using superconducting qubits in Refs. [3,4], both of which contain theoretical analysis that overlaps with ours.

In the absence of driving, the behavior of the system is simple. In the unbiased case (i.e., when $\epsilon_0=0$), the eigenstates of the Hamiltonian are the symmetric and antisymmetric superpositions of the states $|\uparrow\rangle$ and $|\downarrow\rangle$. As a result, if the system is initially in one of these two states, it oscillates back and forth between them. In the strongly biased case (i.e., when $\epsilon_0 \gg \Delta$), the states $|\uparrow\rangle$ and $|\downarrow\rangle$ are, to a good approximation, the eigenstates of the Hamiltonian. If the system is initially in one of them, it will only experience small oscillations, occupying the other state with a maximum probability $(\Delta/\epsilon_0)^2$. One could say that in this case the oscillations, which are driven by the $\hat{\sigma}_x$ term in the Hamiltonian, are suppressed by the energy mismatch ϵ_0 between the states $|\uparrow\rangle$ and $|\downarrow\rangle$.

In the weak driving limit (i.e., when $A \ll \sqrt{\Delta^2+\epsilon_0^2}$), Rabi-oscillation physics applies. Resonance occurs when $\omega = \sqrt{\Delta^2+\epsilon_0^2}$, and the frequency of Rabi oscillations is given by

$\Omega=(A\sin\alpha)/2$, where the angle α is defined by the condition $\tan\alpha=\Delta/\epsilon_0$. Rabi oscillations occur between the eigenstates of the Hamiltonian (excluding the driving term), such that in the unbiased case the oscillations occur between the symmetric and antisymmetric superpositions of the states $|\uparrow\rangle$ and $|\downarrow\rangle$. Higher-order processes, with $n\omega=\sqrt{\Delta^2+\epsilon_0^2}$, can be described easily as well in this limit. We shall collectively refer to the weak-driving limit using the easily recognizable name of Rabi-physics limit.

Since Rabi physics is well known [13], we shall not discuss it in any detail here. Instead, we focus on the case where the amplitude A is comparable to or larger than $\sqrt{\Delta^2+\epsilon_0^2}$. A suitable RWA can be used to obtain a good description of the dynamics when $\omega \gg \Delta$. This approach, described in Sec. III, can explain some interesting features of the problem, in particular the phenomenon of CDT mentioned in Sec. I.

A different approximation can be used when $(A-\epsilon_0) \gg \Delta$ and $A\omega \gg \Delta^2$ (note that this condition overlaps with the validity condition of the RWA). In this case we can think of the dynamics as being composed of a sequence of LZ crossings separated by periods of free evolution of the basis states. We shall take this approach to analyze the problem in Sec. IV. We shall then compare the validity conditions of the different approximations in Sec. V.

III. HIGH-FREQUENCY DRIVING: ROTATING WAVE APPROXIMATION

We now take the system described by the Hamiltonian in Eq. (1) and make a transformation to a rotating frame, such that a wave function $|\psi\rangle$ in the laboratory frame can be expressed as

$$|\psi\rangle = \hat{U}(t)|\psi'\rangle, \qquad (3)$$

where

$$\hat{U}(t) = \exp\left[\frac{i}{2}\left(\epsilon_0 t + \frac{A}{\omega}\sin\omega t\right)\hat{\sigma}_z\right], \qquad (4)$$

and $|\psi'\rangle$ is the wave function in the rotating frame. In other words, we use the interaction picture with the coupling term treated as a perturbation. The Schrödinger equation

$$i\frac{d}{dt}|\psi\rangle = \hat{H}(t)|\psi\rangle \qquad (5)$$

can now be written as

$$i\frac{d}{dt}|\psi'\rangle = \hat{H}'(t)|\psi'\rangle, \qquad (6)$$

with

$$\hat{H}'(t) = \hat{U}^\dagger(t)\hat{H}(t)\hat{U}(t) - i\hat{U}^\dagger(t)\frac{d\hat{U}(t)}{dt}$$

$$= -\frac{\Delta}{2}e^{-(i/2)[\epsilon_0 t + (A/\omega)\sin \omega t]\hat{\sigma}_z}\hat{\sigma}_x e^{(i/2)[\epsilon_0 t + (A/\omega)\sin \omega t]\hat{\sigma}_z}$$

$$= -\frac{\Delta}{2}\begin{pmatrix} 0 & e^{-i[\epsilon_0 t + (A/\omega)\sin \omega t]} \\ e^{i[\epsilon_0 t + (A/\omega)\sin \omega t]} & 0 \end{pmatrix}. \quad (7)$$

We now make use of the relation

$$\exp(iz \sin \gamma) = \sum_{n=-\infty}^{\infty} J_n(z)e^{in\gamma}, \quad (8)$$

where $J_n(x)$ are Bessel functions of the first kind, and we find that

$$\hat{H}'(t) = -\frac{\Delta}{2}\begin{pmatrix} 0 & \sum_{n=-\infty}^{\infty} J_n\left(\frac{A}{\omega}\right)e^{-i(n\omega+\epsilon_0)t} \\ \sum_{n=-\infty}^{\infty} J_n\left(\frac{A}{\omega}\right)e^{i(n\omega+\epsilon_0)t} & 0 \end{pmatrix}. \quad (9)$$

Note that in going from Eq. (1) to Eq. (9) we have not made any approximations. It will be useful below to use the following asymptotic behavior of the Bessel functions:

$$J_n(z) \sim \frac{z^n}{2^n n!}, \quad z \ll 1,$$

$$\quad (10)$$

$$J_n(z) \sim \sqrt{\frac{2}{\pi z}}\cos\left(z - (2n+1)\frac{\pi}{4}\right), \quad z \gg n.$$

We now perform a rotating wave approximation: we assume that all the terms in the sum in Eq. (9) oscillate very fast compared to the time scale of the (coarse-grained, or smoothened) system dynamics, with the exception of one term that is identified as the resonant or near-resonant term. The effect of the nonresonant terms can therefore be neglected when studying the long-time system dynamics. We should note here that this RWA is different from the one widely known and used in the case of weak driving. In that case the linear driving field is replaced by a rotating field, clockwise or counterclockwise depending on conventions. The other component of the field, i.e., the one rotating in the opposite sense, is neglected [14].

The resonance condition is identified using the intuitive requirement that the resonant term of the RWA is constant in time. We therefore have the resonance condition

$$n\omega + \epsilon_0 = 0 \quad (11)$$

for some integer n. With parameters satisfying the resonance condition, the $|\uparrow\rangle \leftrightarrow |\downarrow\rangle$ oscillation frequency is given by
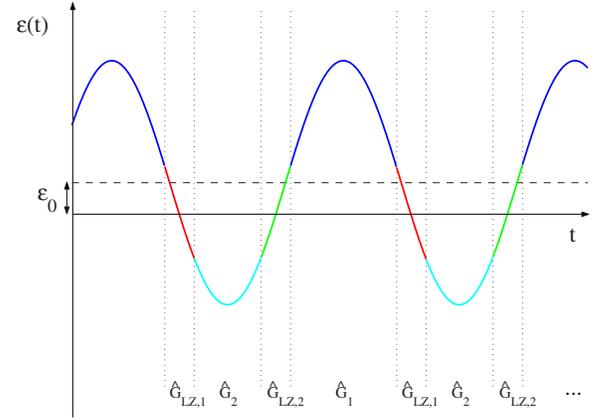
FIG. 2. (Color online) The time evolution of the system divided into discrete time steps, each of which can be described by a simple evolution matrix.

$$\Omega = \Delta\left|J_n\left(\frac{A}{\omega}\right)\right|. \quad (12)$$

One usually identifies the resonance with a given value of n as describing an $|n|$-photon process. The Rabi resonance condition corresponds to the case $n=-1$, where we find that $\omega = \epsilon_0$ (the difference from the condition $\omega = \sqrt{\Delta^2 + \epsilon_0^2}$ will become clear shortly). Assuming weak driving, we find that the frequency of Rabi oscillations is given by

$$\Omega = \frac{\Delta}{\epsilon_0}\frac{A}{2}. \quad (13)$$

For large values of ϵ_0, the factor Δ/ϵ_0 is a good approximation to the factor $\sin \alpha$, where α is the angle between the static bias field and the driving field. The Rabi frequency vanishes asymptotically as $\epsilon_0 \to \infty$, as it should. Note also that Ω [Eq. (12)] increases with increasing A for small values of A, but generally decreases as $1/\sqrt{A}$ for large values of A. The mechanism responsible for this latter behavior will become clear in Sec. IV. In particular, note that the turning point between the two behaviors (or, alternatively, the maximum in Ω) occurs when A is comparable to ϵ_0.

The width of the resonance can be obtained from the following considerations. If the driving frequency is shifted from exact resonance [Eq. (11)] by $\delta\omega$, the resonant (i.e., slowest) term in Eq. (9) oscillates with frequency $n\delta\omega$. When these oscillations become faster than the $|\uparrow\rangle \leftrightarrow |\downarrow\rangle$ oscillation dynamics, which is characterized by Ω, the resonance is clearly lost. The width of the resonance can therefore be taken as

$$\delta\omega \sim \frac{\Omega}{|n|}. \quad (14)$$

Using higher-order processes (i.e., with $|n| > 1$) therefore results in resonances that are narrow compared to the on-resonance oscillation frequency. This property can be useful,
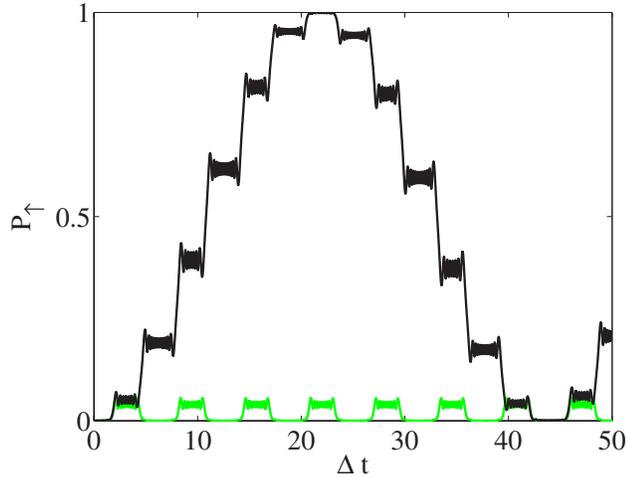
FIG. 3. (Color online) Occupation probability $P_\uparrow$ of the state $|\uparrow\rangle$ as a function of time (in dimensionless units), assuming that the system was initially in the state $|\downarrow\rangle$. We take $\epsilon_0/\Delta = 5$, and $\omega/\Delta = 1$. The driving amplitude is given by $A/\Delta = 30$ for the black line and $A/\Delta = 34.95$ for the green (gray) line (note that the resonance condition is satisfied in both cases). The transfer-matrix method and the RWA of Sec. III both agree well with the numerical results (their predictions are not shown here for clarity).

for example, in applications where one is dealing with several closely spaced resonances. If one is trying to drive only one of those resonances, this approach provides a possibility to target a single resonance, without necessarily making the oscillation dynamics extremely slow.

We now note that for the above resonance condition [Eq. (11)] to hold we must be able to neglect all the oscillating terms. This means that we require that $|n\omega + \epsilon_0| \gg \Delta$ for all n except the one satisfying the resonance condition [15]. Keeping in mind that $|n\omega + \epsilon_0| = 0$ for one value of n, we find that the validity condition can be expressed simply as $\omega \gg \Delta$. This explains the difference between the above resonance condition and the usual resonance condition for Rabi oscillations; for example, when $\epsilon_0 = 0$ and $\omega = \Delta$ we cannot keep only one term in Eq. (9), and this approximation breaks down. Note, however, that even if $\epsilon_0 = 0$ we can still use this approximation, as long as $\omega \gg \Delta$. This approach is very useful when discussing the phenomenon of CDT, which we do next.

The much-analyzed phenomenon of CDT [5] can be explained using the above approach. In the unbiased case (i.e., when $\epsilon_0 = 0$), Eq. (11) gives the interesting result that, regardless of the value of ω, taking $n = 0$ always satisfies the resonance condition. This means that oscillations between the states $|\uparrow\rangle$ and $|\downarrow\rangle$ will always occur with full $|\uparrow\rangle \leftrightarrow |\downarrow\rangle$ conversion, provided of course that we can neglect all the terms with $n \neq 0$ (or in other words $\omega \gg \Delta$). This statement is obvious for no driving ($A = 0$), but it is not obvious that for large driving fields ($A \gg \Delta$) full conversion should occur. From this point of view, it looks more surprising that full oscillations occur at all for strong driving, even though the

system hardly spends any time in the degeneracy region [16]. Accepting the existence of these oscillations, we now take the oscillation frequency as given by Eq. (12) with $n = 0$. It is now clear that CDT occurs when

$$J_0\left(\frac{A}{\omega}\right) = 0, \qquad (15)$$

such that the resonant term in Eq. (9) has a vanishing coefficient [note that Eq. (15) agrees with the results of previous work [5,6]]. With parameters satisfying the CDT condition, the frequency of $|\uparrow\rangle \leftrightarrow |\downarrow\rangle$ oscillations vanishes, and the oscillations are consequently suppressed. One could therefore say that CDT is simply the statement that the $|\uparrow\rangle \leftrightarrow |\downarrow\rangle$ oscillation frequency becomes extremely small if we use driving parameters that are close to a point satisfying Eq. (15).

IV. REPEATED TRAVERSALS OF THE CROSSING REGION: TRANSFER-MATRIX (TM) APPROACH

We now focus on the case of strong driving where the system repeatedly traverses the crossing region [i.e., $(A - \epsilon_0) \gg \Delta$]. Even in the case $\omega \gg \Delta$, where the treatment using the RWA above is still valid, that approach becomes less intuitive. Instead, one can gain better insight into the problem by analyzing the dynamics as composed of finite time steps, as we shall do in this section (see also Ref. [4]).

Let us take the limit where $(A - \epsilon_0) \gg \Delta$. We can now think of the system as undergoing a sequence of LZ crossings. Since we are looking for a resonance condition, we want the LZ transition probability to be small for a single crossing. We therefore assume that each crossing is traversed in the fast limit. This means that we require the sweep rate across the degeneracy region (i.e., $A\omega$ times some geometric factor that depends on ϵ_0/A) to be much larger than the square of the gap size of the crossing Δ^2. Between each two LZ crossings, the system moves far from the degeneracy region and acquires a relative-phase factor between the states $|\uparrow\rangle$ and $|\downarrow\rangle$. Because of the asymmetry (i.e., the fact that, in general, $\epsilon_0 \neq 0$), there are two phase factors corresponding to the system being on the right-hand or left-hand side of the degeneracy region. We therefore find that between crossings, the system evolves by the evolution matrices,

$$\hat{G}_j = \begin{pmatrix} e^{-i\theta_j} & 0 \\ 0 & e^{i\theta_j} \end{pmatrix}, \qquad (16)$$

where j represents the two sides of the degeneracy point (we shall refer to them as 1 and 2). If we approximate the sweep across the degeneracy region by a linear ramp of the bias point between two points located symmetrically around the degeneracy point, we find that the LZ crossing can be approximately described by the evolution matrix,

$$\hat{G}_{\text{LZ},k} = \begin{pmatrix} \cos\dfrac{\chi}{2} & \sin\dfrac{\chi}{2}e^{i\theta_{\text{LZ},k}} \\ -\sin\dfrac{\chi}{2}e^{-i\theta_{\text{LZ},k}} & \cos\dfrac{\chi}{2} \end{pmatrix}, \qquad (17)$$

where the angle χ is defined by the LZ transition probability

$$\sin^2 \frac{\chi}{2} = 1 - \exp\left(-\frac{\pi\Delta^2}{2v}\right) \approx \frac{\pi\Delta^2}{2v}, \qquad (18)$$

v is the sweep rate, and k defines the direction of the bias sweep across the degeneracy region. We do not evaluate $\theta_{LZ,k}$ here for a reason that will become clear below. Note that the sweep rates in the two directions are equal, and thus χ is independent of k. The description of LZ crossing processes using unitary matrices of the form of Eq. (17) is sometimes referred to as the transfer-matrix method, which we follow here (the term scattering matrix can also be found in the literature).

We now have a sequence of finite time steps, each of which is described by a simple evolution matrix, as shown in Fig. 2. The dynamics over a large number of driving cycles can be constructed by multiplying the evolution matrices. The evolution of the system over N cycles is therefore described by the matrix

$$\hat{G}_N = (\hat{G}_{LZ,2}\hat{G}_2\hat{G}_{LZ,1}\hat{G}_1)^N, \qquad (19)$$

with possibly some minor modifications at the beginning and end of the sequence, depending on the exact initial and final bias points [17]. We now take a single cycle and calculate the evolution matrix that describes it. We find that

$$\hat{G}_{LZ,2}\hat{G}_2\hat{G}_{LZ,1}\hat{G}_1 = \begin{pmatrix} g_{11} & g_{21} \\ -g_{21}^* & g_{11}^* \end{pmatrix}, \qquad (20)$$

where

$$g_{11} = \cos^2 \frac{\chi}{2} e^{-i(\theta_1+\theta_2)} - \sin^2 \frac{\chi}{2} e^{i(-\theta_{LZ,1}+\theta_{LZ,2}-\theta_1+\theta_2)},$$

$$g_{21} = \sin \frac{\chi}{2} \cos \frac{\chi}{2} (e^{i(\theta_{LZ,1}+\theta_1-\theta_2)} + e^{i(\theta_{LZ,2}+\theta_1+\theta_2)}). \qquad (21)$$

It is useful to rewrite Eq. (20) as

$$\hat{G}_{LZ,2}\hat{G}_2\hat{G}_{LZ,1}\hat{G}_1 = \begin{pmatrix} \cos \dfrac{\zeta_{FC}}{2} & \sin \dfrac{\zeta_{FC}}{2} e^{i\phi_{FC}} \\ -\sin \dfrac{\zeta_{FC}}{2} e^{-i\phi_{FC}} & \cos \dfrac{\zeta_{FC}}{2} \end{pmatrix}$$
$$\times \begin{pmatrix} e^{-i\theta_{FC}/2} & 0 \\ 0 & e^{i\theta_{FC}/2} \end{pmatrix}, \qquad (22)$$

where the subscript FC indicates that the above equation describes the evolution of the system over a full cycle of the driving field. We now find that

$$\sin^2 \frac{\zeta_{FC}}{2} \approx 4 \sin^2 \frac{\chi}{2} \cos^2\left(\frac{\theta_{LZ,1}-\theta_{LZ,2}}{2} - \theta_2\right),$$

$$\theta_{FC} = 2 \arctan \frac{\cos^2 \chi/2 \sin(\theta_1+\theta_2) + \sin^2 \chi/2 \sin(\theta_{LZ,1}-\theta_{LZ,2}+\theta_1-\theta_2)}{\cos^2 \chi/2 \cos(\theta_1+\theta_2) - \sin^2 \chi/2 \cos(\theta_{LZ,1}-\theta_{LZ,2}+\theta_1-\theta_2)} \approx 2(\theta_1+\theta_2), \qquad (23)$$

$$\phi_{FC} \approx \frac{\theta_{LZ,1}+\theta_{LZ,2}}{2} - \theta_2.$$

We can now analyze the dynamics described by Eq. (22). The first matrix in the product describes a rotation by a small angle ζ_{FC} around an axis in the xy plane. The second matrix in the product describes a rotation by an angle θ_{FC} around the z axis. The resonance condition now becomes clear. If θ_{FC} is a multiple of 2π, the z-axis rotation does not affect the dynamics, and the small rotations of ζ_{FC} add up to produce full oscillations between the states $|\uparrow\rangle$ and $|\downarrow\rangle$. If, on the other hand, θ_{FC} takes a value that is different from any multiple of 2π by more than ζ_{FC}, the small rotations of ζ_{FC} will not add

up in an ideal manner, and the oscillations will be suppressed [19]. The resonance condition for the above constructive accumulation of small rotations can be obtained by noting that

$$\theta_{FC} \approx 2(\theta_1+\theta_2) \approx \int_\tau^{\tau+2\pi/\omega} dt(\epsilon_0 + A\cos\omega t) = \frac{2\pi\epsilon_0}{\omega}. \qquad (24)$$

The resonance condition is therefore given by

$$\frac{\epsilon_0}{\omega} = n \tag{25}$$

for some integer n. This is the same condition that we found in Sec. III, using an entirely different approach (note also that the validity conditions of the two approaches are different, a point to which we shall come back in Sec. V).

Using the approach of this section it might seem somewhat surprising that the amplitude A does not appear in the resonance condition, even though A can be the largest energy scale in the problem. One should also note here that Eq. (11) is only approximate in the weak-driving limit, with a correction that is proportional to A^2 (i.e., the Bloch-Siegert shift). One might therefore expect that such corrections will take over at some point, such that the amplitude A becomes an essential part of the resonance condition. Counterintuitively, however, these corrections change behavior and vanish asymptotically for large A. The fact that the two (identical) resonance conditions are good approximations deep in opposite limits demonstrates further that the derivation of Eq. (25) in this section should not be thought of as simply a rederivation of Eq. (11). It is worth noting here that even for nonharmonic driving we can follow a similar analysis to what was done in this section and find that the resonance condition is still independent of the driving amplitude, with ϵ_0 replaced by the time-averaged value of the bias point and ω replaced by 2π over the driving period [see Eq. (24)].

The frequency of oscillations on resonance can now be obtained directly. If we assume that the resonance condition in Eq. (25) is satisfied, we find that the $|\uparrow\rangle \leftrightarrow |\downarrow\rangle$ oscillation frequency is given by

$$\Omega = \frac{\omega \zeta_{FC}}{2\pi} \approx \frac{2\omega}{\pi} \sin\frac{\chi}{2} \left| \cos\left(\frac{\theta_{LZ,1} - \theta_{LZ,2}}{2} - \theta_2 \right) \right|. \tag{26}$$

Note that since the value of θ_2 depends on where we set the boundaries between the different time steps, the same must be true about $\theta_{LZ,1}$ and $\theta_{LZ,2}$. In order to simplify the expressions below, we use instead of θ_2, $\theta_{LZ,1}$, and $\theta_{LZ,2}$ boundary-independent phase factors $\tilde{\theta}_2$, $\tilde{\theta}_{LZ,1}$, and $\tilde{\theta}_{LZ,1}$. We now define $\tilde{\theta}_2$ as the phase accumulated between the times of level crossings (pretending in this evaluation that the $\hat{\sigma}_x$ coupling term is absent). With this definition of $\tilde{\theta}_2$, we find that the appropriate values of $\tilde{\theta}_{LZ,1}$ and $\tilde{\theta}_{LZ,2}$ are given in terms of the so-called Stokes phase θ_{Stokes} [18],

$$\tilde{\theta}_{LZ,1} = \frac{\pi}{2} + \theta_{Stokes},$$

$$\tilde{\theta}_{LZ,2} = \frac{\pi}{2} - \theta_{Stokes},$$

$$\theta_{Stokes} = \frac{\pi}{4} + \Gamma(1 - i\delta) + \delta(\ln\delta - 1), \tag{27}$$
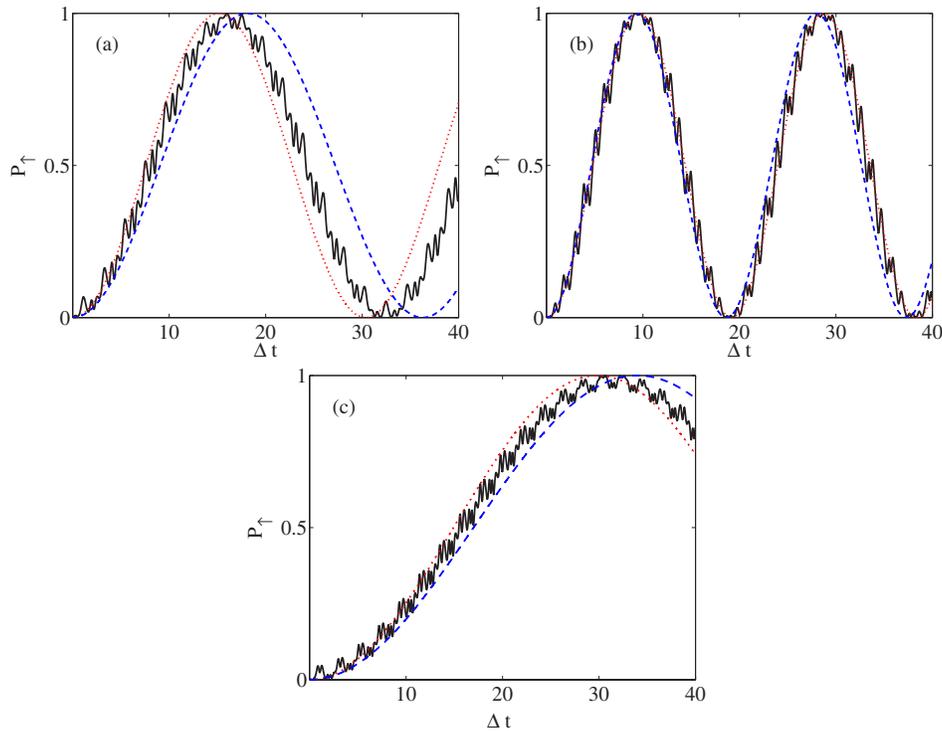
FIG. 4. (Color online) Occupation probability $P_\uparrow$ of the state $|\uparrow\rangle$ as a function of time (in dimensionless units), assuming that the system was initially in the state $|\downarrow\rangle$. In all the figures $\epsilon_0/\Delta = \omega/\Delta = 3$. The driving amplitude is given by $A/\Delta = 10$ (a), 15 (b), and 20 (c). The blue dashed line gives the (coarse-grained) predicted dynamics from the transfer-matrix method in the large-amplitude limit, and the red dotted line gives the predicted dynamics from Sec. III.
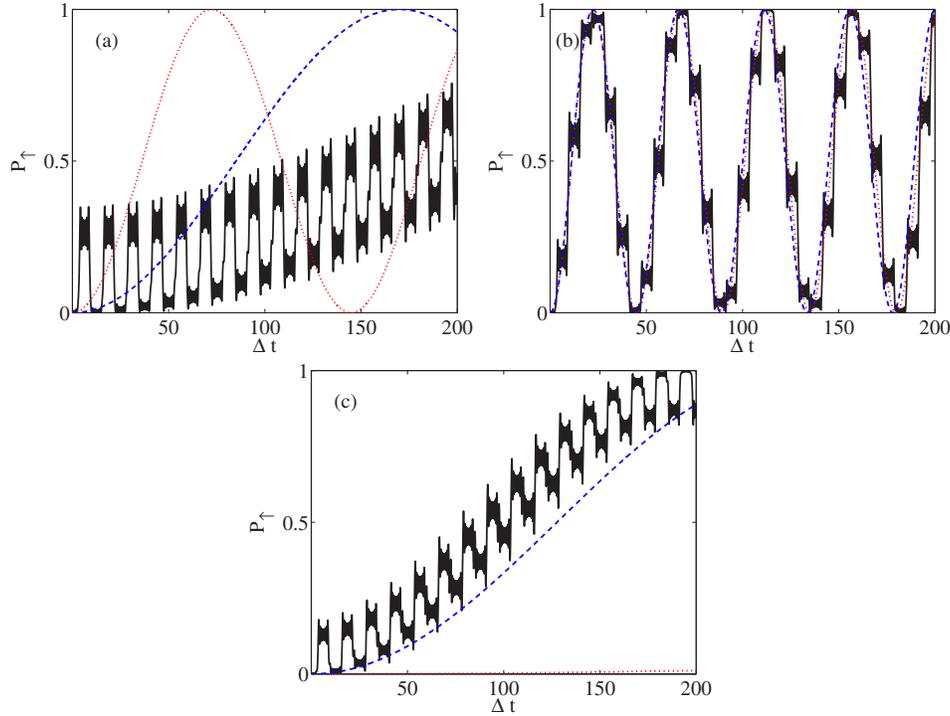
FIG. 5. (Color online) Occupation probability $P_\uparrow$ of the state $|\uparrow\rangle$ as a function of time (in dimensionless units), assuming that the system was initially in the state $|\downarrow\rangle$. In all the figures, $\epsilon_0/\Delta=1$, and $\omega/\Delta=0.5$. The driving amplitude is given by $A/\Delta=12$ (a), 16 (b), and 20 (c). The blue dashed line gives the (coarse-grained) predicted dynamics from the transfer-matrix method in the large-amplitude limit, and the red dotted line gives the predicted dynamics from Sec. III.

$$\delta = \frac{\Delta^2}{4v},$$

and $\Gamma(x)$ is the gamma function. Note that θ_{Stokes} approaches the value $\pi/4$ in the fast-crossing limit (i.e., when $\delta \to 0$). We therefore find that

$$\Omega \approx \frac{2\omega}{\pi} \sqrt{\frac{\pi\Delta^2}{2\omega\sqrt{A^2 - \epsilon_0^2}}} |\cos(\widetilde{\theta}_2 - \theta_{\text{Stokes}})|. \quad (28)$$

The phase $\widetilde{\theta}_2$ can be calculated as

$$\widetilde{\theta}_2 = \frac{\sqrt{A^2 - \epsilon_0^2}}{\omega} - \frac{\epsilon_0}{\omega} \cos^{-1} \frac{\epsilon_0}{A}. \quad (29)$$

In the special case $\epsilon_0 = 0$, we find that $\widetilde{\theta}_2 = A/\omega$, and using the fact that $\theta_{\text{Stokes}} \approx \pi/4$ we recover Eq. (12) with $n=0$ for the oscillation frequency.

One might wonder why several expressions above are not symmetric with respect to θ_1 and θ_2. This asymmetry results from our grouping of evolution matrices into full cycles [see Eq. (19)], as well as the order of matrices in Eq. (22). These are clearly matters of convention. Different orderings of the matrices can result in different-looking expressions. The end result must of course be independent of this choice. For example, if we substitute Eq. (29) into Eq. (28), we do not see any convention dependence.

In order to illustrate the transfer-matrix picture, we show in Figs. 3–5 numerical simulations of the dynamics in the

validity region of that picture. We plot the occupation probability of the state $|\uparrow\rangle$ as a function of time, assuming that the system was initially in the state $|\downarrow\rangle$. We can see in Fig. 3 that the occupation probability exhibits sudden jumps that correspond to LZ crossings. The steps are rather large in this figure because the crossings are not in the fast limit. If we look on long time scales, we can see that the dynamics looks like sinusoidal oscillations. This long-time behavior becomes particularly smooth when the transition probability in a single LZ crossing is small, as is the case in Fig. 4. We also plot in Figs. 4 and 5 sinusoidally oscillating functions with frequencies given by Eq. (28) [20], as well as sinusoidally oscillating functions with frequencies given by Eq. (12) from Sec. III. In Fig. 5 the driving frequency ω is smaller than Δ. We therefore find inconsistency in the predictions of Eq. (12). As a general rule, the RWA gives reasonable or good agreement with the numerical simulations when the resulting oscillation frequency in the system dynamics is large. When the oscillation frequency is small, the effect of the resonant term is not necessarily large compared to that of the other terms in Eq. (9), and the RWA fails. This is most clearly seen in Fig. 5(c). In Fig. 4, we are in the region where $\omega > \Delta$, and we always find that both Eq. (12) and Eq. (28) agree well with the numerical simulations.

The fact that the resonance condition is always satisfied in the unbiased case is very clear in this approach. In this case, the phase factors θ_1 and θ_2 accumulated on the two sides cancel because of symmetry, regardless of the driving amplitude and frequency.
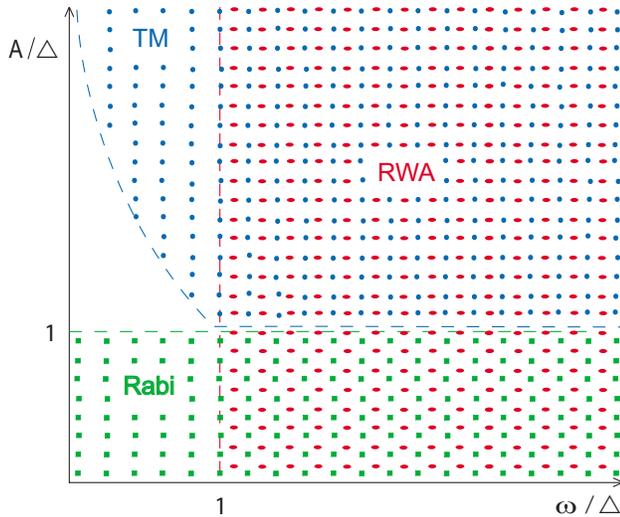
FIG. 6. (Color online) Regions of validity for different approximations. TM stands for transfer-matrix method, RWA stands for the rotating wave approximation presented in this paper, and Rabi stands for the weak-driving limit best known in connection with Rabi oscillations. The axes are the frequency ω and amplitude A of the driving field, both normalized to the minimum gap Δ. The Rabi region is described by the condition $A/\Delta < 1$ (regardless of the value of ω), and it is shown by green squares. The RWA region is described by the condition $\omega/\Delta > 1$, and it is shown by red ellipses. The TM region is described by the conditions $A/\Delta > 1$ and $A\omega > \Delta^2$, and it is shown by blue circles. Note that ϵ_0 was generally assumed to be comparable to Δ in this figure.

The factor $|\cos(\tilde{\theta}_2 - \theta_{\text{Stokes}})|$ in Eq. (28) gives a nontrivial dependence of the $|\uparrow\rangle \leftrightarrow |\downarrow\rangle$ oscillation frequency on the bias and driving parameters. It lies behind the phenomenon that even if the resonance condition is satisfied, it is still possible for the oscillations to be so slow that the resonance is effectively destroyed (see Fig. 3). In other words, it describes the same mechanism responsible for CDT, and it agrees with the Bessel ladder structure discussed in Ref. [3].

The width of the resonance can be obtained as explained above. We require that the phase factor θ_{FC} be within a distance ζ_{FC} from a multiple of 2π. Starting from Eq. (24), and writing

$$\theta_{\text{FC}} \approx 2\pi n - \frac{2\pi\epsilon_0}{\omega^2}\delta\omega, \tag{30}$$

where $\delta\omega$ is the deviation from exact resonance, we find that the width of the resonance is given by

$$\delta\omega \sim \frac{\omega^2 \zeta_{\text{FC}}}{2\pi\epsilon_0} \sim \frac{\Omega}{n}. \tag{31}$$

As in Sec. III, we find that in addition to the usual factor of oscillation frequency, the width of the resonance now contains the factor $1/n$. This means that with the proper choice of parameters, the width of the resonance can be made substantially smaller than the on-resonance oscillation frequency.

V. DISCUSSION AND CONCLUSION

In this paper we have presented two approaches to study the problem of a strongly driven two-level system. The first one (presented in Sec. III) was based on a rotating wave approximation, whereas the second one (presented in Sec. IV) was based on a discretized description of the dynamics. It is important to note that the two approaches have different regions of validity, as shown in Fig. 6. We also include in Fig. 6 the region of validity for the weak-driving limit, which is most clearly associated with Rabi physics. As can also be seen in Fig. 6, the different regions overlap substantially, and two of them can sometimes be used to describe the same situation. For example, although the derivation and the appearance of the results of Sec. IV rely strongly on the picture of LZ crossings, the results agree with those of Sec. III whenever $\omega \gg \Delta$. Naturally, the deeper one goes into one of these regions, the better results one can expect to obtain from the corresponding approximation.

The regions not covered by any of the approximations in Fig. 6 do not necessarily correspond to drastically different physical mechanisms. For example, the dynamics shown in Fig. 5(a) with low-frequency, large-amplitude driving corresponds to a point that lies close to the boundary between the TM region and the unshaded region, such that none of the approximations presented here gives accurate results in this case. The dynamics in that figure contain a large transition probability between the two basis states in a single crossing. However, this case can be conceptually understood using the same picture as in the transfer-matrix approach discussed here.

An example of simple dynamics that corresponds to points in the unshaded region occurs in the large-amplitude, slow-crossing limit. In a single crossing, the system follows the energy eigenstates almost adiabatically (i.e., with small mixing between the energy eigenstates in a single crossing). We obtain simple resonance dynamics in this case as well. However, the resonance dynamics now describes oscillations between the (time-dependent) energy eigenstates, rather than between the states $|\uparrow\rangle$ and $|\downarrow\rangle$.

The approaches discussed here therefore cover a large portion of the parameter space. They provide alternative points of view for understanding the mechanisms at play in the dynamics of this system [21]. It is worth noting that the approach of Sec. IV is not limited to harmonic driving. It can be used to treat any system with large-amplitude driving around the degeneracy point, assuming the approximation of linear sweeps through the crossing region is valid [22].

Experiments on two-level systems have generally suffered from short coherence times. With the advent of the field of QIP, the need for long coherence times has spurred a fast advance in the direction of isolating qubits from their environments, thus resulting in relatively long coherence times. For example, high-order processes and quantum interference between LZ crossings have already been observed in superconducting qubit systems [3,4,23,24]. One could in the future realistically think about using strong driving as a tool to manipulate qubits. The mechanisms discussed in this paper can be used in constructing such qubit-manipulation tools.

[1] See, e. g., M. A. Nielsen and I. L. Chuang, *Quantum Computation and Quantum Information* (Cambridge University Press, 2000); J. Stolze and D. Suter *Quantum Computing: A Short Course from Theory to Experiment* (Wiley, Weinheim, 2004).

[2] L. D. Landau, Phys. Z. Sowjetunion **1**, 88 (1932); **2**, 46 (1932); C. Zener, Proc. R. Soc. London, Ser. A **137**, 696 (1932); E. C. G. Stueckelberg, Helv. Phys. Acta **5**, 369 (1932); E. Majorana, Nuovo Cimento **9**, 43 (1932).

[3] W. D. Oliver, Y. Yu, J. C. Lee, K. K. Berggren, L. S. Levitov, and T. P. Orlando, Science **310**, 1653 (2005); D. M. Berns, W. D. Oliver, S. O. Valenzuela, A. V. Shytov, K. K. Berggren, L. S. Levitov, and T. P. Orlando, Phys. Rev. Lett. **97**, 150502 (2006).

[4] M. Sillanpää, T. Lehtinen, A. Paila, Y. Makhlin, and P. Hakonen, Phys. Rev. Lett. **96**, 187002 (2006).

[5] F. Grossmann, T. Dittrich, P. Jung, and P. Hänggi, Phys. Rev. Lett. **67**, 516 (1991); F. Grossmann and P. Hänggi, Europhys. Lett. **18**, 571 (1992).

[6] Y. Kayanuma, Phys. Rev. B **47**, 9940 (1993); Phys. Rev. A **50**, 843 (1994).

[7] B. M. Garraway and N. V. Vitanov, Phys. Rev. A **55**, 4418 (1997).

[8] M. Grifoni and P. Hänggi, Phys. Rep. **304**, 229 (1998).

[9] C. E. Creffield, Phys. Rev. B **67**, 165301 (2003).

[10] The Floquet theory for periodically driven systems has been applied to this problem extensively as well. See, e.g., W. Magnus and S. Winkler, *Hill's Equation* (Dover, New York, 1966).

[11] Another related problem that displays interesting features is that of a system traversing an avoided-crossing region while being driven by an oscillating field: Y. Kayanuma and Y. Mizumoto, Phys. Rev. A **62**, 061401(R) (2000); S. Q. Duan, L. B. Fu, J. Liu, and X. G. Zhao, Phys. Lett. A **346**, 315 (2005); M. Wubs, K. Saito, S. Kohler, Y. Kayanuma, and P. Hänggi, New J. Phys. **7**, 218 (2005).

[12] Here we treat the $\hat{\sigma}_z$ term as the externally tunable term, and we use the eigenstates of $\hat{\sigma}_z$, to which we refer as $|\uparrow\rangle$ and $|\downarrow\rangle$, as the preferred basis in our analysis.

[13] See, e.g., G. Baym, *Lectures on Quantum Mechanics* (Addison Wesley, New York, 1990).

[14] The usual RWA can also be described using the same reasoning used here. Starting from the initial Hamiltonian and after some algebra, one obtains an equation of motion with terms that oscillate with frequencies $\omega \pm \sqrt{\epsilon_0^2 + \Delta^2}$. The terms that oscillate with frequency $\omega + \sqrt{\epsilon_0^2 + \Delta^2}$ are then neglected on the basis of their fast oscillations. See, e.g., C. W. Gardiner and P. Zoller, *Quantum Noise* (Springer, Heidelberg, 2004).

[15] Note that, in order to achieve simpler appearance, we have dropped the Bessel functions from the right-hand side of the inequality, because they are generally of order 1. This explains why we shall find cases where $\omega < \Delta$, but the RWA still gives good agreement with the exact results.

[16] From Eq. (10), with $z \gg n$, we can see that the frequency of $|\uparrow\rangle \leftrightarrow |\downarrow\rangle$ oscillations scales as $\sqrt{\omega/A}$, apart from the cosine factor. The larger the driving amplitude (within a certain region), the slower the oscillations, in agreement with our intuitive guess.

[17] The $|\uparrow\rangle \leftrightarrow |\downarrow\rangle$ oscillation dynamics occurs on a much longer time scale than $1/\omega$, such that the exact details of the boundary conditions do not have a significant impact on the dynamics.

[18] See, e. g., M. V. Berry, in *Asymptotics Beyond All Orders*, edited by H. Segur and S. Tanveer (Plenum, New York, 1991).

[19] In fact, starting from Eq. (22) one can use straighforward geometric arguments to show that the evolution of the system over a full driving cycle in the nonresonant case can be represented by a single rotation about an axis that is almost parallel to the z axis. This means that we cannot obtain $|\uparrow\rangle \leftrightarrow |\downarrow\rangle$ oscillations by repeated application of this rotation.

[20] Note that the TM approach can also be used to obtain the steplike dynamics of this system. However, here we only show coarse-grained sinusoidally oscillating functions for clarity.

[21] Furthermore, our results could help understand the behavior of other systems. For example, results with features similar to those of our results were obtained in the study of transport in periodic potentials; J. Rotvig, A. P. Jauho, and H. Smith, Phys. Rev. Lett. **74**, 1831 (1995); Phys. Rev. B **54**, 17691 (1996).

[22] Recently there have been some results on LZ crossings using non-linear ramps; F. Gaitan, Phys. Rev. A **68**, 052314 (2003); P. Földi, M. G. Benedict, J. Milton Pereira, Jr., and F. M. Peeters, Phys. Rev. B **75**, 104430 (2007).

[23] See also Y. Nakamura, Y. A. Pashkin, and J. S. Tsai, Phys. Rev. Lett. **87**, 246601 (2001); A. Wallraff, T. Duty, A. Lukashenko, and A. V. Ustinov, *ibid.* **90**, 037003 (2003); S. Saito, M. Thorwart, H. Tanaka, M. Ueda, H. Nakano, K. Semba, and H. Takayanagi, *ibid.* **93**, 037001 (2004); A. Izmalkov, M. Grajcar, E. Il'ichev, N. Oukhanski, T. Wagner, H.-G. Meyer, W. Krech, M. H. S. Amin, A. Maassen van den Brink, and A. M. Zagoskin, Europhys. Lett. **65**, 844 (2004); C. M. Wilson, T. Duty, F. Persson, M. Sandberg, G. Johansson, and P. Delsing, e-print arXiv:cond-mat/0703629.

[24] For recent reviews, see e.g., J. Q. You and F. Nori, Phys. Today **58**(11), 42 (2005); G. Wendin and V. Shumeiko, in *Handbook of Theoretical and Computational Nanotechnology*, edited by M. Rieth and W. Schommers (ASP, Los Angeles, 2006).